Available online at www.sciencedirect.com
SCIENCE DIRECT®
Planetary and Space Science 53 (2005) 395–412
Planetary and Space Science
www.elsevier.com/locate/pss

Are Io's Alfvén wings filamented? Galileo observations

T. Chust[a,*], A. Roux[a], W.S. Kurth[b], D.A. Gurnett[b], M.G. Kivelson[c], K.K. Khurana[c]

[a]*Centre d'étude des Environnements Terrestre et Planétaires, UMR 8639, CNRS-UVSQ, 10-12 Avenue de l'Europe, F-78140, Vélizy, France*
[b]*Department of Physics and Astronomy, UI, Iowa City, IA 52242, USA*
[c]*Institute of Geophysics and Planetary Physics, UCLA, Los Angeles, CA 90024, USA*

Received 26 November 2003; received in revised form 28 June 2004; accepted 15 September 2004

Abstract

The interaction of Io with the Jovian magnetosphere generates auroral and radio emissions. The underlying electron acceleration process is not understood and few observations exist to constrain the theoretical models. The source of energy for the electron acceleration is in all likelihood supplied from the Alfvén wings that stretch out from both poles of Io into the two Jovian hemispheres. The form of the current system associated with the Alfvén wings has been disputed, some suggesting that the greatly slowed flow near Io implies that a steady current loop links Io to Jupiter's ionosphere, others arguing that the return waves appear only downstream of Io and others suggesting that both forms develop. Given the finite inclination of the Alfvén wings implied by the finite value of the Alfvén Mach number and the strong reflection that occurs at the boundary of the Io torus, we argue that no steady current loop can be invoked between Io and Jupiter's ionosphere. However, the energetics of the auroral and radio emissions imply that most of the energy in the Alfvén wings is transformed into electron acceleration at high-latitudes, that is, outside the Io torus. The dilemma then is to understand how a large fraction of the power penetrates the reflecting boundary. We present data from Galileo's multiple flybys of Io that suggest that the coupling with the Jovian ionosphere is mediated by filamentary Alfvén wings associated with electromagnetic waves propagating out of the torus. In particular, we report on the systematic observation, within the cross-section of Io's Alfvén wings and in their immediate vicinity, of intense electromagnetic waves at frequencies up to several times the proton gyrofrequency. We interpret these "high-frequency/small-scale" waves as the signature of a strong filamentation/fragmentation of the Alfvén wings before they reflect off of the sharp boundary gradient of the Io torus. As a consequence, we suggest that most of the primary energy is converted into "high-frequency/small-scale" electromagnetic waves that can propagate out from the torus toward Jupiter's ionosphere. Reaching high-latitudes, these waves are able to accelerate electrons to almost relativistic speeds.

Keywords: Alfvén wing; Filamentation; Electron acceleration; Wave propagation; Inhomogeneity; Io–Jupiter interaction

1. Introduction

The existence of a non-thermal radio emission controlled by Io is well documented (Bigg, 1964; Warwick, 1981; Zarka et al., 1996, 2001; Queinnec and Zarka, 1998). While the exact mechanism producing the shape of the Io-related decametric arcs is not fully understood, it is generally accepted that the cyclotron maser instability is the basic excitation mechanism for these non-thermal radio emissions. It has been suggested that the atmospheric loss cone provides the free energy source for the cyclotron maser instability. In order to explain the correlation between the radio emissions and the location of Io, the size of the loss cone must be enhanced in the Io flux tube and in its trailing edge in the sense of flow (which corresponds to the orbital leading side of Io because Jupiter rotates faster than Io does).

*Corresponding author. Fax: +33 1 3925 4922.
E-mail addresses: thomas.chust@cetp.ipsl.fr (T. Chust), wsk@space.physics.uiowa.edu (W.S. Kurth), mkivelson@igpp.ucla.edu (M.G. Kivelson).

0032-0633/$ - see front matter © 2004 Elsevier Ltd. All rights reserved.
doi:10.1016/j.pss.2004.09.021

An enhanced loss cone can be produced by a parallel potential drop along the flux tube. Another free energy source can be considered. Noting that the Io-associated emissions are similar to terrestrial auroral kilometric radiation (AKR), we can expect that the same mechanism is operating at both planets. The observations made by Viking (Louarn et al., 1990) and later by FAST (Delory et al., 1998) have shown that the electron distribution function in the AKR source region is a horse-shoe shaped distribution, which is unstable to the maser cyclotron instability. This horse-shoe distribution can result from a combination of the mirror force and a time-varying parallel potential drop (Louarn et al., 1990). In any case, energetic electrons (of the order of a few keV), reaching Jupiter's ionosphere at about 10–25° longitude ahead of the unperturbed Io flux tube (in the sense of planetary rotation) and representing a power of the order of 10^{11} W (Queinnec and Zarka, 2001) (assuming a 10% power transfer coefficient from particle to radiation), are directly involved in producing the Io-related decametric arcs.

More recently, some of the Jovian auroral emissions have been identified as the magnetic footprint of Io (Connerney et al., 1993; Prangé et al., 1996, 1998; Vasavada et al., 1999; Clarke et al., 1996, 1998). The measurements of these Io-related auroras have been made over a wide spectral range, from the infrared to the far ultraviolet, including visible light. These auroras consist of spot-like emissions detected in both hemispheres at the latitude of the magnetic foot-points of Io; their longitudinal locations are variable, with lead angles ranging from about 0° to 20° with respect to the unperturbed Jupiter's magnetic field line connected to Io. Their size is of the order of 200–500 km which roughly corresponds to the projection of Io onto Jupiter's upper atmosphere, or a little more. A very faint and narrow trail following the Io-related spot in the sense of planetary rotation and forming almost an entire oval has also been detected. It brightness decreases as the distance from the Io footprint increases. These Io-related auroral emissions imply a power input varying from about $1–5 \times 10^{11}$ W per hemisphere. These observations collectively place quantitative constraints on the properties of the source region near Io, and in this paper we exploit them in developing an interpretation of the plasma–Io interaction.

Io's interaction is modeled as that of a conducting body moving through a magnetized plasma. This interaction generates electromagnetic waves that radiate away (Drell et al., 1965; Neubauer, 1980, 1998; Wright and Schwartz, 1990). The waves have a typical frequency given by v_0/L, where v_0 is the velocity of the moving source (in the reference frame of the plasma) and L is its size along the direction of motion. Isotropic modes are damped because they spread out as they propagate away from the source. Guided modes form "wings" or "tubes" that stretch out from both sides of the body along their characteristics. In general, boundaries exist in the wave medium and reflected wings may overlap. The relative intensity associated with each mode depends on the boundary conditions. In the case of Io, estimates based on MHD simulations suggest that most of the energy generated goes into the Alfvén mode rather than into the fast and slow magnetosonic modes (Linker et al., 1988, 1991). In situ magnetic field measurements from Voyager 1 have given evidence for a $\sim 3 \times 10^6$ A, bipolar, standing Alfvén wave current system that closes through Io and/or its ionosphere (Acuna et al., 1981; Neubauer, 1980). The source of this current system is the jovian corotation electric field, which is $\simeq 0.1$ V/m at Io. The short-circuiting by Io implies that a power of the order of 10^{12} W is radiated away into each Alfvén wave current tube (Io's diameter is about 3650 km, but the effective short-circuit size is probably slightly larger due to the ionosphere and to the pickup currents). Note that a finite conductivity may dissipate an important fraction of this power into Joule heating (Saur et al., 1999). However, the remaining power is still of the order of or slightly above the total power needed for producing the auroral and radio emissions described above.

The first models of the electrodynamic interaction between Io and Jupiter were developed at a time when the properties of Io's atmosphere and its dense plasma torus were not known. As a result, Alfvén disturbances generated at Io were believed to propagate up to the Jovian ionosphere and to be reflected back on a time scale very short in comparison with the convection time of the plasma past Io. Thus, a steady current loop was thought to form. The classic unipolar inductor model (Piddington and Drake, 1968; Goldreich and Lynden-Bell, 1969; Hill et al., 1983), which couples Io to the Jovian ionosphere, is indeed obtained as the extreme case of an infinite number of overlapping reflected Alfvén wings (Neubauer, 1998). In fact, the round-trip travel time of an Alfvén disturbance from Io to the Jovian ionosphere (mainly spent within the dense torus) is of the order of 1000 s (Hill et al., 1983; Crary and Bagenal, 1997), which is much larger than the typical "excitation" time ($L/v_0 \sim 60$ s) of the Jovian magnetospheric field lines by the motion of Io. Furthermore, because of the strong increase of the Alfvén speed at the torus boundary, most of the power in the Alfvén wing must be reflected (Wright and Schwartz, 1989; Crary, 1997) and cannot reach the Jovian ionosphere. The unipolar inductor model can therefore not be the relevant model. However, after Galileo observed strongly slowed plasma flow within the Alfvén wings (Frank et al., 1996; Frank and Paterson, 2001, 2002), the unipolar inductor model was resurrected (e.g., Crary and Bagenal, 1997; Hill and Pontius, 1998). We believe that the arguments used to support this model are based

on erroneous considerations previously proposed (Goldreich and Lynden-Bell, 1969; Goertz and Deift, 1973; Hill et al., 1983): In these papers, the condition for the reflected Alfvén wings to overlap is based on the slow speed of the perturbed plasma past Io instead of the nominal (unperturbed) flow velocity (v_0). First, the perturbed flow results from the self-consistent electrodynamic interaction between Io and Jupiter and cannot, therefore, be considered as the excitation source of the global Alfvén wing disturbance. Within the Alfvén wing, the plasma flow can be approximately at rest with respect to Io, but in this case it will be about twice as fast as the nominal flow outside the Alfvén wing, on the equatorial flanks. Nevertheless, there is only one "excitation" time that characterizes the Alfvén wing disturbance, which is given by the nominal convection time of the unperturbed plasma past Io (L/v_0). This can be most easily seen in the reference frame of the plasma where the Alfvén wing disturbance propagates along the unperturbed Jovian magnetic field lines, after having been launched from Io. Second, it is incorrect to extrapolate equatorward Alfvén characteristics of a pure incident wing up to the reflecting layer. The exact non-linear (asymptotic) solution of an upward Alfvén wing disturbance given by Neubauer (1980) shows precisely that the downward Alfvén characteristics within the wing are not parallel to those defined outside, which leads to a puzzling situation since the Alfvén disturbance has to reflect in its entirety. For instance, in the case of a strong interaction (vanishing electric field within the Alfvén wing and twice its nominal value on its flanks), the equatorward Alfvén characteristics within the wing are strongly distorted from their nominal direction and are parallel to the axis of the Alfvén wing; outside, they are also strongly distorted but in the opposite direction. Indeed, the non-linear coupling between the incident and reflected wings has to be taken into account; it involves compressional modes, so that the equatorward Alfvén characteristics in the vicinity of the reflecting layer are connected with the nominal equatorward Alfvén characteristics. As a result, the geometry of the reflection of an Alfvén wing is determined from the nominal (Jupiterward and equatorward) Alfvén characteristics and hence simply from the Alfvén Mach number (the ratio between v_0 and the Alfvén speed), independently of the perturbation intensity of the plasma flow. Thus, we believe that the pure Alfvén wing model (no significant overlapping) is the relevant zero order model of the electromagnetic interaction between Io and Jupiter. This model will be adopted hereafter as the initial framework for the analysis developed below.

The high-latitude phenomena, the aurora and non-thermal radio emissions, require intensified fluxes of energetic electrons at or near the Io flux tube. It is clear that the source of energy originates from the sweeping of Io by the plasma of the jovian magnetosphere, and that this interaction leads to the formation of an Alfvén wave current system/Alfvén wing. The energy budget discussed above implies that a large fraction of the current density in the Alfvén wings goes into accelerating electrons. However, the mechanism by which the wave energy is transferred to the electrons is not understood. Several mechanisms have been proposed to transform the magnetic energy in the Alfvén wings into particle energy (e.g., Crary, 1997; Kopp et al., 1998; Das and Ip, 2000), but there is no consensus yet, as illustrated here above and discussed later on. The Galileo spacecraft made a number of low altitudes passes near Io and the fields/particles instruments have collected new information. In the present paper we take advantage of the systematic observation during these flybys of intense electromagnetic waves at frequencies up to several times the local proton gyrofrequency. We use this unique opportunity, together with particle data collected during these flybys, to identify new constraints and help understand how the electromagnetic energy in the Alfvén wave current system is transformed into particle acceleration.

2. Galileo observations

2.1. Overview of the plasma wave observations

Galileo measured plama waves on six flybys of Io. The corresponding orbits are labeled I0, I24, I25, I27, I31, and I32. Fig. 1 shows the trajectories of the Galileo spacecraft during these flybys in the Io frame of reference. The relative speed v_0 between Io and the unperturbed magnetospheric flow is ~57 km/s. The altitudes of closest approach are 897, 611, 300, 198, 193 and 184 km, respectively. The I0 flyby was a downstream wake pass, the I25 and I32 flybys were south polar passes, I31 flyby was a north polar pass, and the I24 and I27 flybys were upstream passes in the anti-Jupiter flank region. Figs. 2–7 show for each pass the calibrated dynamic power spectra of the waves measured by the Galileo Plasma Wave Subsystem (PWS, Gurnett et al., 1992). The frequency range covers 5.4 Hz to 5.6 MHz for the electric spectra (top panels) and 5.4 Hz to 160 kHz for the magnetic spectra (bottom panels). The spectrum analyzer toggles between the electric and magnetic antennas every 18.666 s. These spectra are obtained via several logspaced filters having different frequency resolution, depending on their central frequencies. The vertical widths of the rectangular color patterns are proportional to the frequency resolution.

The I25 spectra have been computed from realtime science data that have been compressed/decompressed; there are uncertainties in the amplitudes in these data.

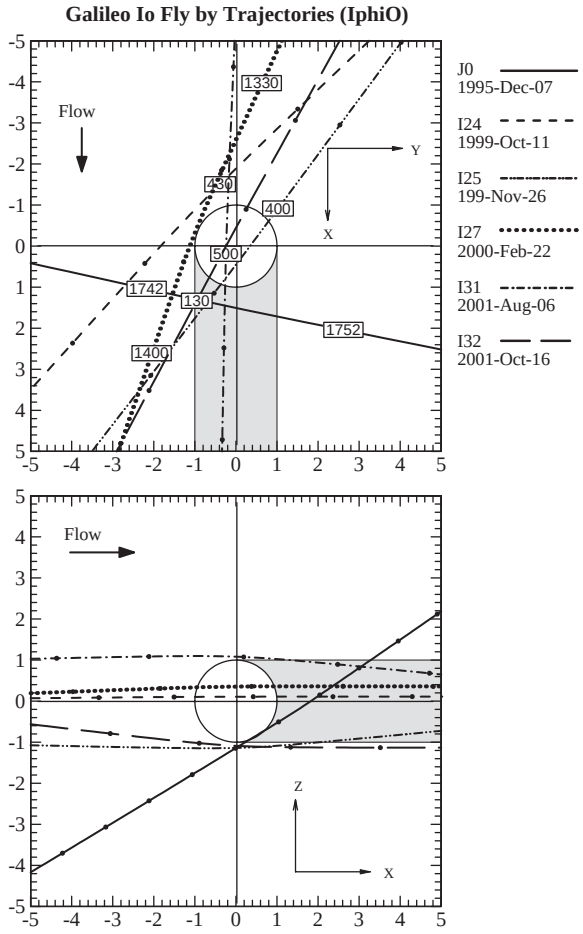

Fig. 1. The trajectories of the Galileo spacecraft during the I0, I24, I25, I27, I31, and I32 flybys, in the Io-centric IphiO coordinate system (the x-axis is parallel to the unperturbed flow, the y-axis is pointing toward Jupiter, and the z-axis is parallel to Jupiter's spin axis). They are shown with time ticks or boxes every 10 min.

All other spectra have been computed from full resolution low rate science playback data that have not been compressed. These other data, therefore, have more reliable amplitudes. However, since day 277 of year 1997 the electronics of the magnetic antenna have suffered from a malfunction that reduces the measured power spectral density by a constant factor. We will show later on that this constant is about 10^5. If the resulting magnitude of the magnetic signal is below the noise, the information is lost. If not, that is, for very intense signals, multiplication by 10^5 gives the right order of magnitude. The I0 data that are not affected by the problem will be used as a reference to measure the wave amplitudes. Also clearly visible on these magnetic data is a straight line at ~42 Hz arising from instrumental noise.

The fine spectral line observed on the electric component at $3–5 \times 10^5$ Hz and above is interpreted as emissions at the upper hybrid resonance frequency. Being close to the electron plasma frequency, this line permits one to compute the electron density profile along the Galileo trajectory. More details can be found in Gurnett et al. (2001). A large increase in the plasma density is measured: (1) in the middle of the wake at a relatively large distance from the surface of Io (a peak density of about $4 \times 10^4\,\mathrm{cm}^{-3}$ is found during the I0 flyby), (2) over the poles within a broad region that seems to correspond to the whole cross-section of Io's unperturbed flux tube shifted in the downstream direction (peak density of about $2 \times 10^4\,\mathrm{cm}^{-3}$, during the I25 flyby, and similar values for the I31 and I32 flybys) and, (3) at the closest approach during the I27 flyby (peak density of about $7 \times 10^4\,\mathrm{cm}^{-3}$). No plasma density variation is observed during the I24 flyby. Correspondingly, intense bursts of broadband low frequency electromagnetic wave emissions are observed for the I0, I25, I27, I31 and I32 flybys, whereas no similar wave emission is observed for the I24 flyby. All flybys, except the I24 flyby, present similar observations. The geometry of the flybys suggests that the density and wave intensity increases occur whenever the Galileo spacecraft crosses field lines connected to the ionosphere of Io. Indeed, during the I24 flyby, the Galileo spacecraft did not cross any field lines connected to the ionosphere of Io, whereas during the other flybys it did cross them.

2.2. Observations from other Galileo instruments

Observations obtained from other Galileo instruments provide important context for the interpretation of PWS observations.

2.2.1. The I0 pass

For the I0 flyby, the PWS burst of wave emissions is observed from about 17:45:47 to 17:47:20 UT, that is, in a narrow region approximately centered around the middle of the wake, where the Galileo's Plasma Analyser (PLS) directly observed a cold, dense (consistent with PWS result), and near-stagnant plasma (<1 km/s) (Frank et al., 1996). Simultaneously, intense magnetic field-aligned, bidirectional, electron beams were observed with the Energetic Particle Detector (EPD, >15 keV) (Williams et al., 1996, 1999; Mauk et al., 2001) and with the PLS instrument (>8 eV) (Frank and Paterson, 1999). The pitch angle half width of these beams is estimated to be $\sim 6^\circ$ and the temperature inferred from the single phase-space-density spectrum is about 300 eV. The intensity spectrum measured along the magnetic field direction has a smooth peak at about 300 eV and corresponds to an energy flux of about $7 \times 10^{-4}\,\mathrm{W/m^2}$.

Measurements from the Magnetometer, at 0.22 s resolution, also reveal a strong interaction between Io and the flowing plasma of the Io torus (Kivelson et al.,

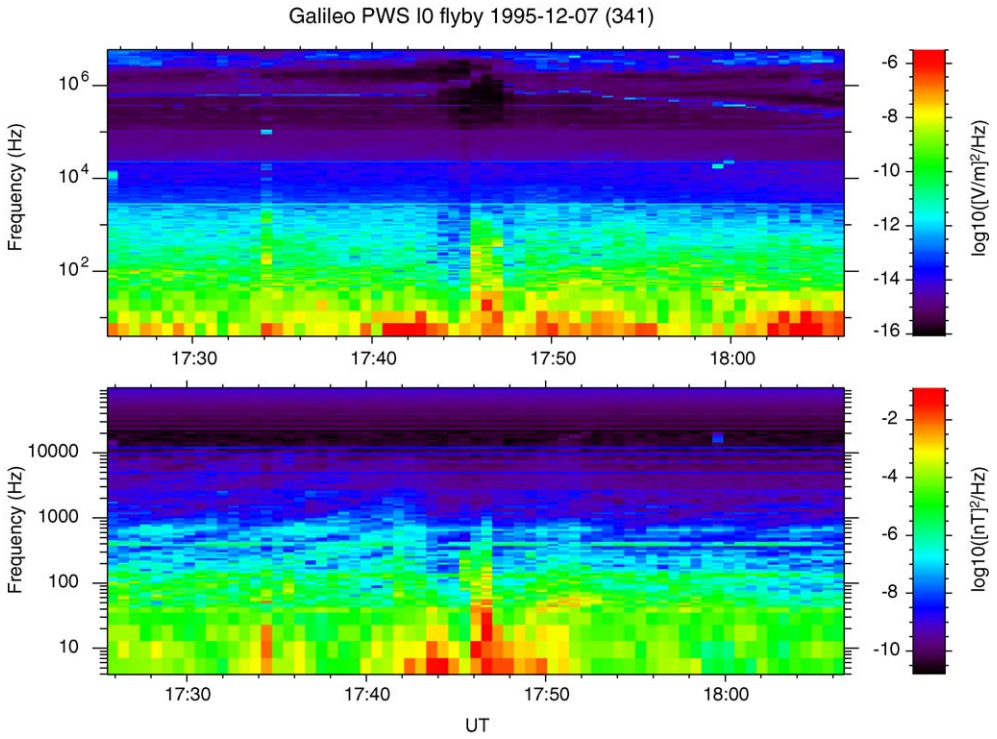

Fig. 2. Calibrated dynamic power spectra of the waves as Galileo flew through the Io wake during the I0 flyby. The top (bottom) panel shows the data from the electric (magnetic) antenna. The closest approach occurred just before 17:46 UT.

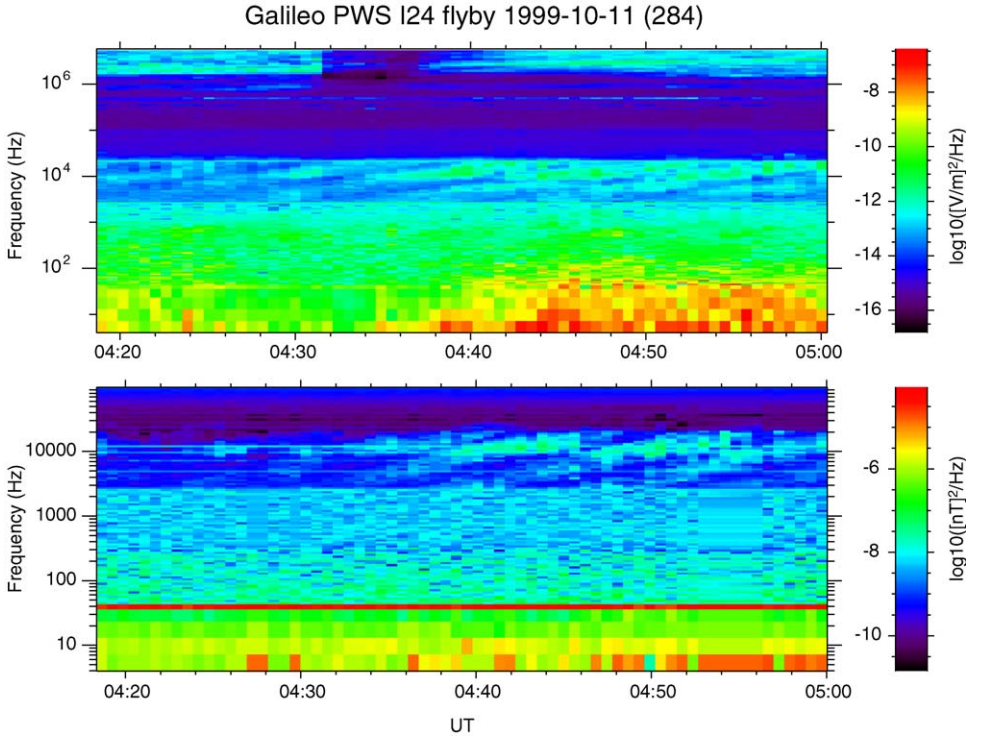

Fig. 3. Same as Fig. 2 but for the upstream I24 flyby. The closest approach occurred at 04:33:03 UT.

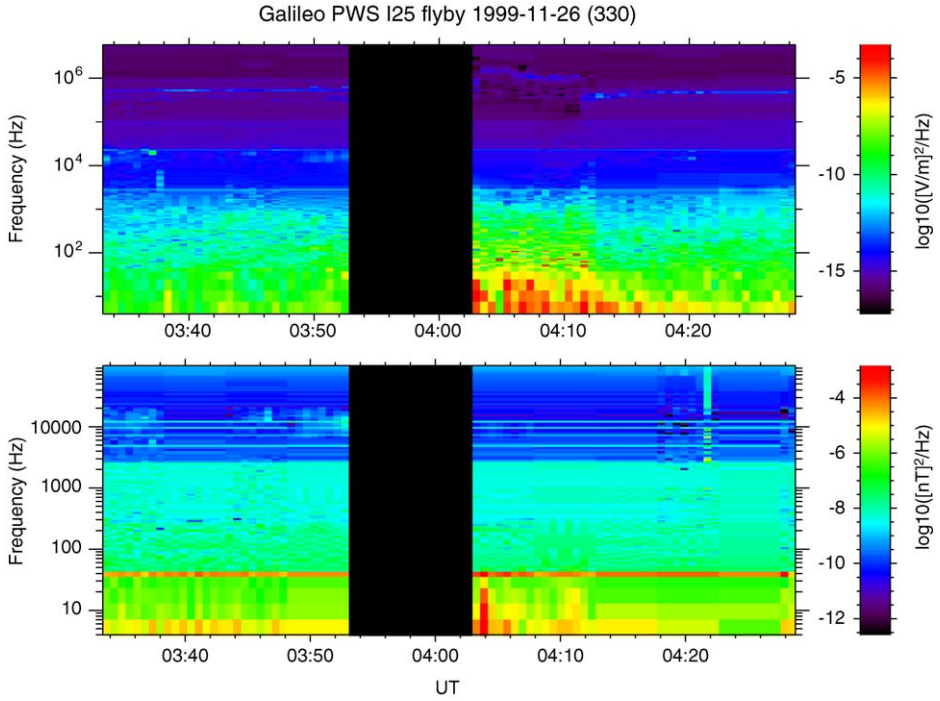

Fig. 4. Same as Fig. 2 but for the south polar I25 flyby. The closest approach occurred at 04:05:21 UT.

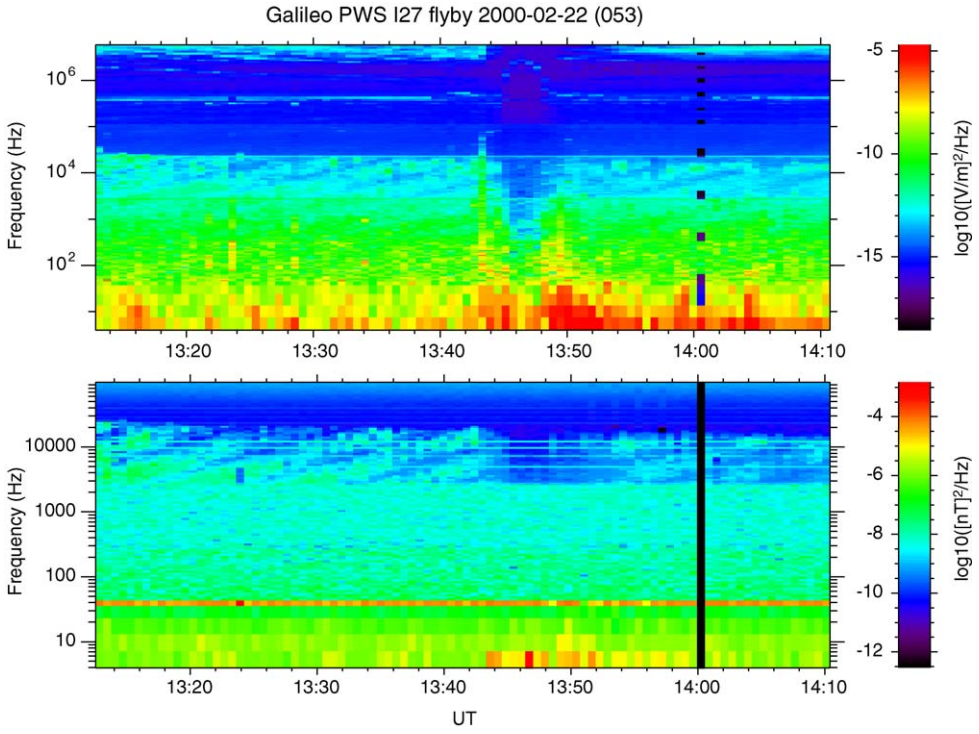

Fig. 5. Same as Fig. 2 but for the upstream I27 flyby. The closest approach occurred at 13:46:41 UT.

1996a,b, 2001a). We reproduce in Fig. 8 the three magnetic field components observed during the (geometrical) wake crossing. The left panel shows a global view while the right panel presents a blow-up of the wake region. At the outer edge of the cold wake, strong compressional fluctuations interpreted as mirror-mode structures have been observed (Kivelson et al., 1996b; Huddleston et al., 1999; Russell et al., 1999), while farther from the wake ion cyclotron waves driven by heavy iogenic molecular pickup ions (sulfur dioxide and

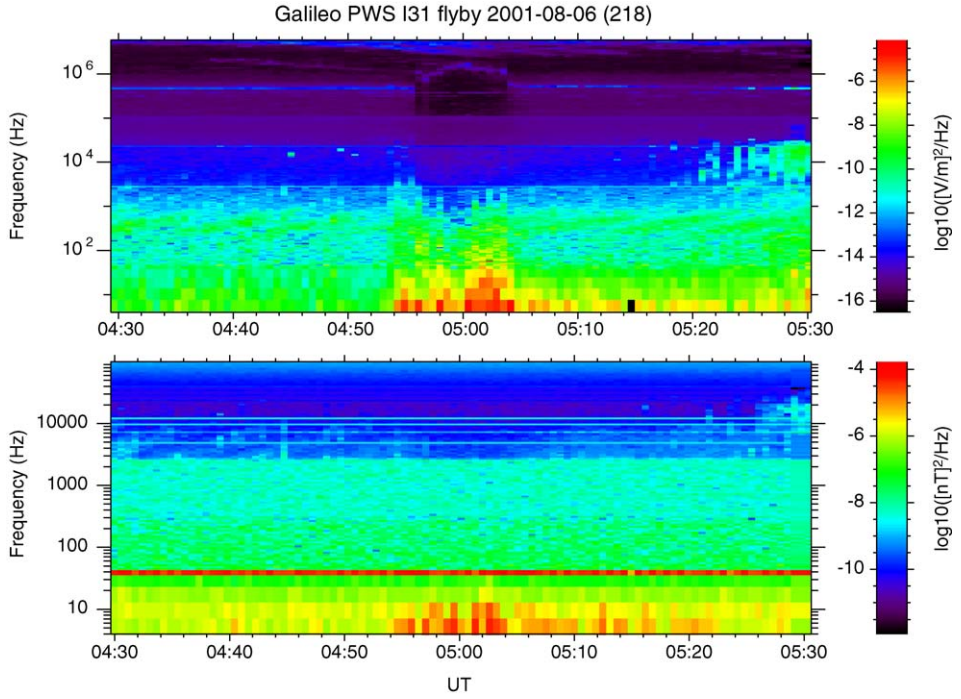

Fig. 6. Same as Fig. 2 but for the north polar I31 flyby. The closest approach occurred at 04:59:20 UT.

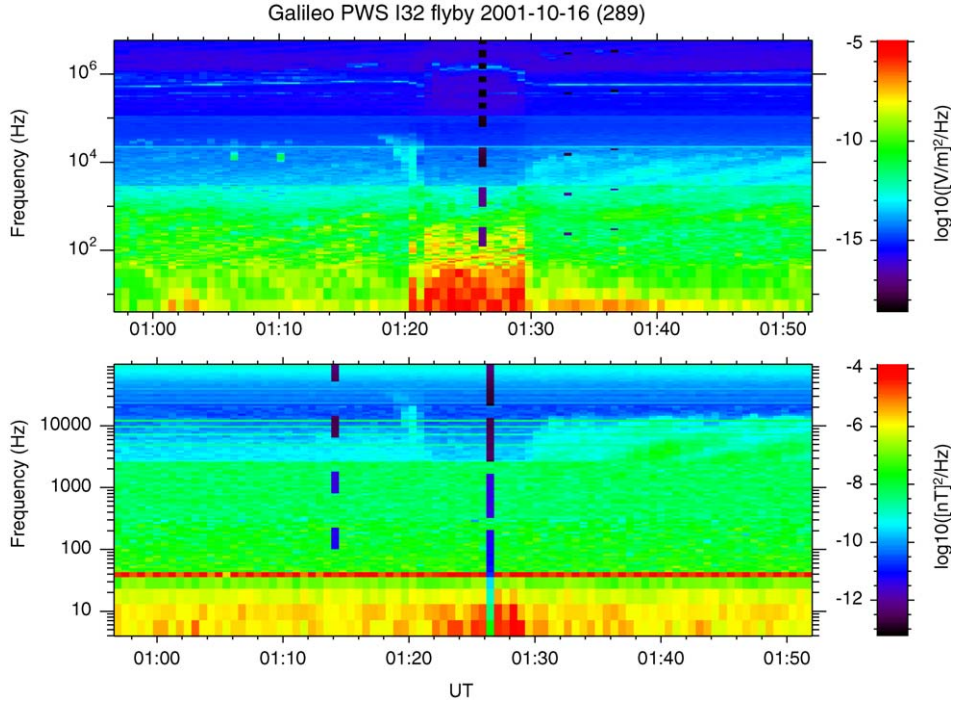

Fig. 7. Same as Fig. 2 but for the south polar I32 flyby. The closest approach occurred at 01:23:21 UT.

sulfur monoxide, mainly) have been observed (Kivelson et al., 1996b; Warnecke et al., 1997; Huddleston et al., 1997, 1998); at higher frequencies, electromagnetic waves driven unstable by iogenic pickup protons have also been observed with the PWS instrument (Chust et al., 1999). In the cold, near-stagnant wake, small-scale incompressible magnetic fluctuations are observed. These magnetic fluctuations observed from the magnetometer are weak in comparison to the mirror-mode structures but distinctly present. They have

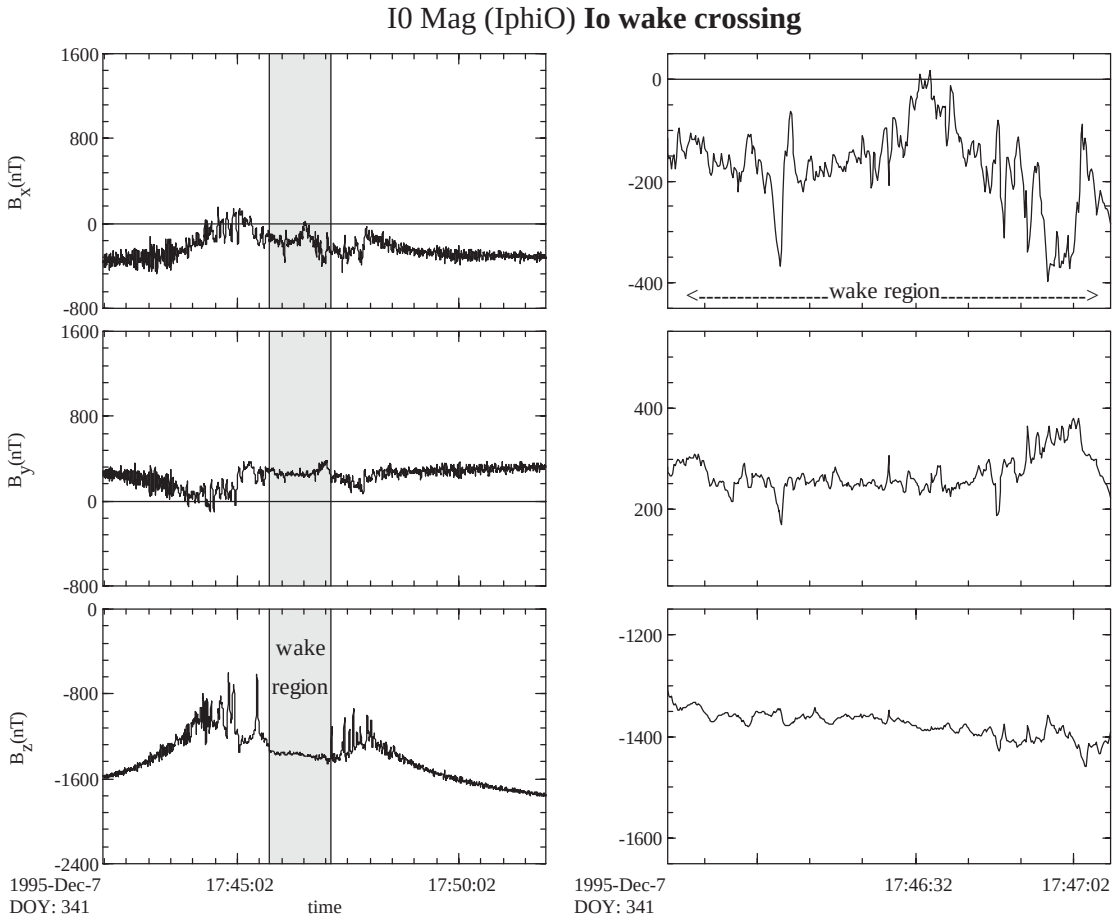

Fig. 8. Magnetometer data during the I0 flyby in the Io-centric IphiO coordinate system (the x-axis is parallel to the unperturbed flow, the y-axis is pointing toward Jupiter, and the z-axis is parallel to Jupiter's spin axis). The left panel gives an overview of the wake crossing and the right panel presents the blow-up of the wake region that is gray colored.

amplitudes as large as 140 nT and are observed over time scales as small as 2 s, which means scale lengths as small as 30 km, if we interpret the variations observed in the frame of the spacecraft as Doppler-shifted spatial structures.

2.2.2. *The polar passes*

The I25 burst of wave emissions occurs over a much longer time interval than for I0, namely from about 4:02:58 to 4:12:18 UT, which corresponds to the crossing of the south Alfvén/sonic wing. Because of delayed recovery from a spacecraft data acquisition gap, no data from the particle instruments and the magnetometer were recorded during this time.

During the two other polar flybys, I31 and I32, the same phenomenon is observed: a burst of intense wave emissions is clearly visible inside a region corresponding to the cross-section of Io. This occurs from about 4:54:13 to 5:04:11 UT and 1:20:34 to 1:29:17 UT, respectively, that is, where the magnetometer observes a large magnetic field perturbation (in particular in the downstream component) which is characteristic of the crossing of an Alfvén wing (Kivelson et al., 2001b). The bursts of wave emissions observed during the I31 and I32 flybys are thus observed within the north and south Alfvén wings, respectively, if not within a slightly wider region extending from the outer edge of the actual Alfvén wings. This result confirms that the I25 burst of wave emissions does correspond to the crossing of the south Alfvén wing. Furthermore, the measurements from the magnetometer during these two polar flybys reveal that within the Alfvén wings, important small-scale incompressible magnetic fluctuations (as large as 150 nT and over scale lengths as small as few tens of kilometers much like the fluctuations observed on I0 and plotted in Fig. 8) exist (Kivelson et al., 2001b). Fig. 9 shows the magnetometer data during the I31 pass. As for the I0 pass in the wake, the high-frequency ($\geqslant 5$ Hz) plasma wave emissions, reported here within the Alfvén wings, are observed together with low frequency ($\leqslant 2$ Hz) Alfvénic fluctuations or small-scale field aligned currents.

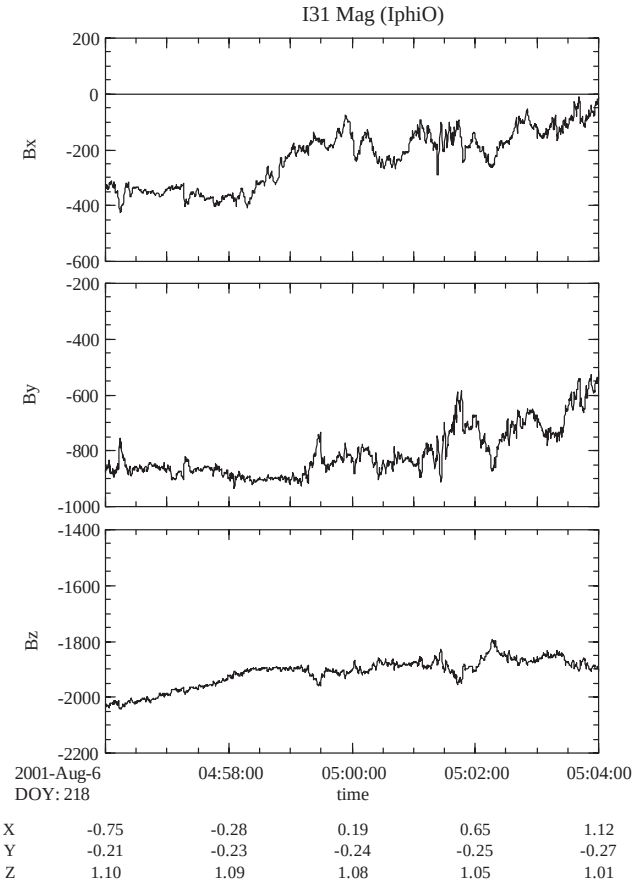

Fig. 9. Magnetometer data during the I31 flyby in the same coordinate system as in Fig. 8: Blow-up of the crossing of the northern Alfvén wing.

Over the northern polar cap during the I31 flyby, the PLS instrument observes a near stagnant plasma (Frank and Paterson, 2002), as it did in the middle of the Io wake during the I0 flyby. The observations are consistent with a highly conductive path through Io or a conducting ionosphere needed for the closure of the Alfvén wing currents. The PLS instrument also observes enhanced field-aligned electrons (Paterson and Frank, 2002a,b). The EPD instrument observes unidirectional beams of energetic electrons and ions, streaming toward Io (Mauk, 2001).

2.2.3. *The upstream equatorial passes*

During the I27 pass two bursts of wave emissions are observed, one just before the closest approach (at ~13:46:30 UT), from about 13:43:20 to 13:45:13 UT, the second one just after, from about 13:48:20 to 13:50:11 UT. In contrast to the polar and wake passes, these wave emissions are remarkably anti-correlated with small-scale incompressible magnetic fluctuations (here as large as 100 nT and again over time scales of the order of 2 s) that are present just in the interval between the bursts (Kivelson et al., 2001a). An intensification of the magnetic fluctuations is however observed in the middle of this interval (see the red spot at the first frequency channel of the magnetic spectra). The anti-correlation thus concerns only the electric field fluctuations and not the magnetic fluctuations. The two distinct wave bursts, separated by the gap in electric wave emission, have the same spectral shape as the waves observed in the wake (I0 flyby) and above the poles (I25, I31 and I32 flybys). Thus they are likely to have the same origin. In fact, we will interpret the plasma wave emissions observed in the immediate vicinity of Io environment as the signature of electromagnetic waves generated inside the Alfvén wings, at some distance from Io, that propagate along the field lines connected to Io. Also, the particular feature of the wave spectra observed at the closest approach will be interpreted as the effect of a large plasma density increase on the wave propagation. Unlike the I0, I31 and I32 passes no electron beam was observed by the EPD instrument during the I27 pass (Mauk et al., 2001). Instead a strong decrease in electron intensities was observed, from about 13:45:00 to 13:48:30 UT, that is, approximately during the time interval where the electric field of the broadband electromagnetic wave emissions decreases and the low frequency ($\leqslant 2$ Hz) incompressible magnetic fluctuations develop. The depletion in energetic electrons occurred when Galileo was very close to Io and is probably due to collisions with the increasingly dense plasma, as one gets closer to Io; or to shadowing effects since Galileo may encounter field lines connected to Io's ionosphere. The PLS instrument observed there a plasma velocity almost at rest with respect to Io ($\simeq 2$ km/s) and a very low plasma temperature (Frank and Paterson, 2001). The trajectory of Galileo being off the equatorial plane of Io, one can understand why this decrease in the flux is larger for electrons coming from the direction of the equatorial plane than for electrons coming from the opposite direction. On the other hand, when a gap in the wave electric spectra and a depletion in energetic electron are observed, the PLS data give evidence for the presence of an electron beam (W. Paterson and L. Frank, private communication, 2002). As shown latter on, our interpretation can account for this observation.

During the I24 flyby, measurements from the magnetometer (Kivelson et al., 2001a) and the PLS instrument (Frank and Paterson, 2000) show a large-scale variation of the magnetic field and the plasma flow, respectively, that are associated with the Alfvén wings at Io. On the other hand, no small-scale incompressible magnetic fluctuations are observed and the measurements from the EPD instrument (Mauk et al., 2001) show no obvious response to the presence of Io. Thus, it has been concluded from these observations that the Galileo spacecraft flew past the Io Alfvén wave current system but did not cross the field lines connected to Io's

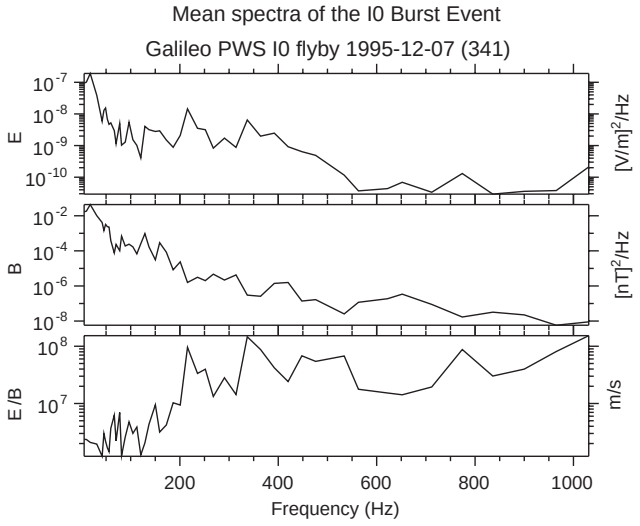

Fig. 10. Electric and magnetic wave spectra averaged over the I0 burst (two top panels, respectively) and the corresponding E over B ratio (bottom panel).

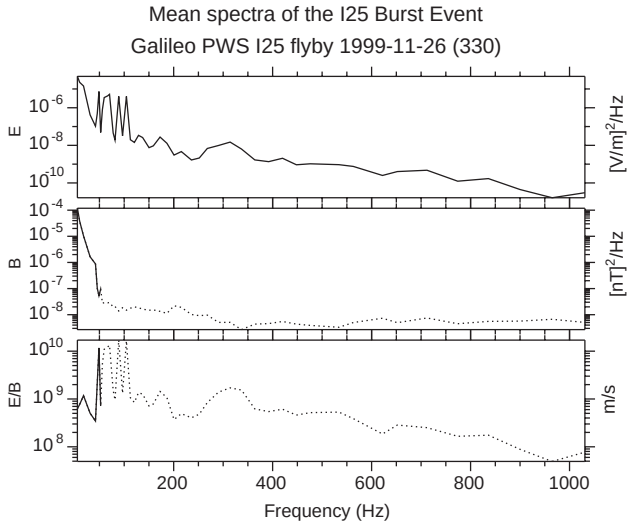

Fig. 11. Same as Fig. 10 but for the south polar I25 flyby.

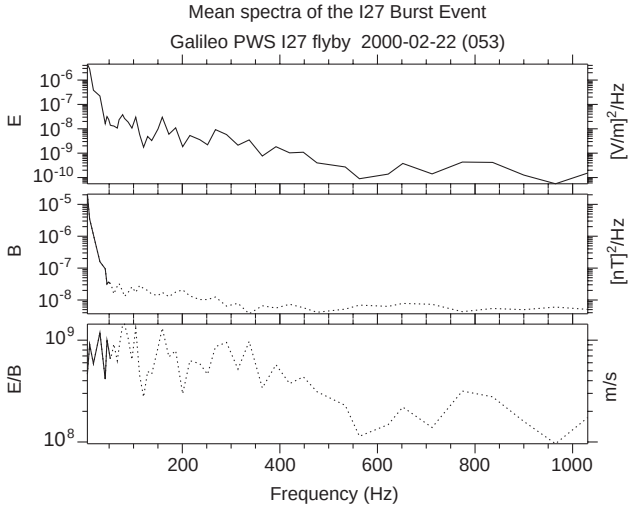

Fig. 12. Same as Fig. 10 but for the upstream I27 flyby.

ionosphere which carry the most intense currents that close through the Io's environment. This is consistent with the conclusion drawn from the plasma wave observations: The Galileo spacecraft did not cross any field line connected to Io's ionosphere during the I24 flyby.

2.3. Analysis of the PWS spectra for the burst events

Fig. 10 shows the electric and magnetic wave spectra averaged over the burst in the I0 pass (two top panels, respectively) and the corresponding E over B ratio (bottom panel). The frequency range displayed is from 5 to 1000 Hz. The magnetic spectrum contains two sharp decreases, the first one around 60 Hz (about twice the proton gyrofrequency) and a second at about 200 Hz. Most of the magnetic energy is contained below 60 Hz ($\simeq 96.7\%$), the rest of the energy being essentially below the second cutoff at about 200 Hz. The electric spectrum also displays a decrease around 60 Hz but only $\sim$76% of the energy is contained below 60 Hz. An increase in the spectral intensity is observable between 200 and 400 Hz. The E over B ratio gives further evidence that waves are predominately electromagnetic below 200 Hz and electrostatic above. The integration over the frequencies of the electric and magnetic power spectral densities gives $(\delta E)^2 \simeq 4.9 \times 10^{-6}\,(\mathrm{V/m})^2$ and $(\delta B)^2 \simeq 0.86\,\mathrm{nT}^2$, respectively. The integrated Poynting flux can also be computed over the whole frequency range, which gives a flux intensity of about $1.5 \times 10^{-6}\,\mathrm{W/m^2}$. Using the "effective" wave amplitudes,

$$F_{\mathrm{P}} = \frac{\delta E\,\delta B}{\mu_0} \tag{1}$$

gives an approximate flux intensity that is very close to the integrated one. Similarly,

$$R_{E/B} = \frac{\delta E}{\delta B} \tag{2}$$

gives a numerical value of $\sim 2 \times 10^6\,\mathrm{m/s}$ which is the typical value computed for the part of the spectrum lying below 60 Hz. This is consistent with the fact that most of the energy is contained in a relatively narrow frequency band, from 5 Hz to approximately 60 Hz. Notice that the low frequency limit given here (5 Hz) is instrumental. A large fraction of the wave energy is below 5 Hz but cannot be measured from the PWS instrument. Measurements from the magnetometer confirm this interpretation.

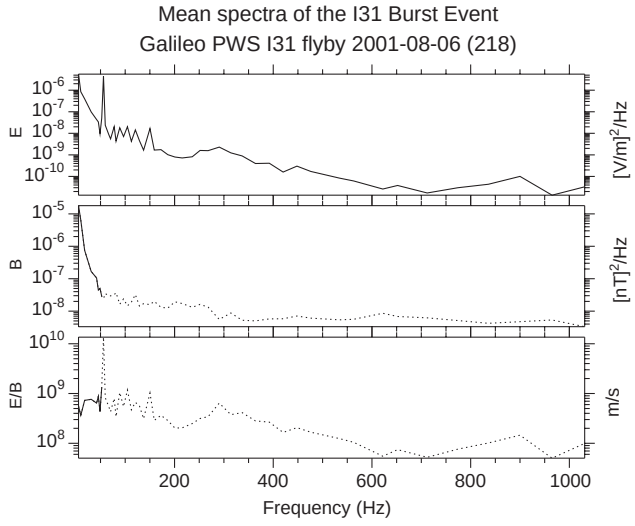

Fig. 13. Same as Fig. 10 but for the north polar I31 flyby.

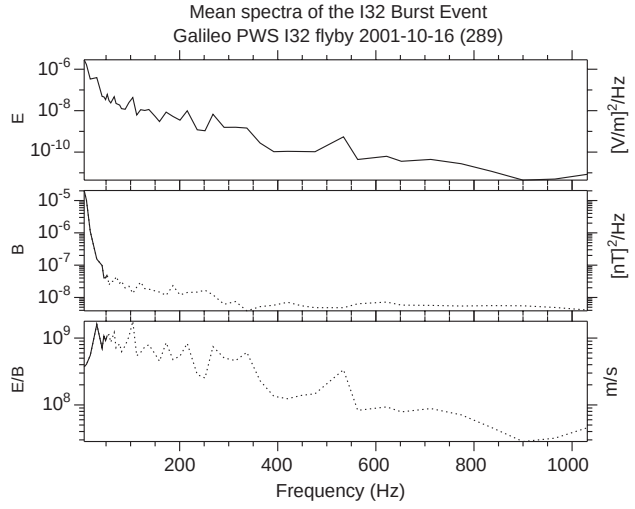

Fig. 14. Same as Fig. 10 but for the south polar I32 flyby.

In the same format as the previous figure, Figs. 11–14, show the electric and magnetic wave spectra averaged over the I25, the two I27, the I31 and the I32 bursts, respectively, and the corresponding E over B ratios. For the magnetic spectra, the spurious line at ~42 Hz has been filtered out. Also, it has to be stressed that a portion of the frequency range that is displayed is not meaningful for the magnetic data and thus for the E over B ratio. The corresponding data are indicated by dotted curves. As explained above, owing to a failure in the electronic processing of the magnetic signal, the effective sensitivity of the magnetic antenna is severely decreased. In fact, the four curves of the magnetic spectra displayed in the middle panels of Figs. 11–14, respectively, are very similar for frequencies greater than about 50 Hz. We conclude that this part of the spectra (>50 Hz) is obscured by spurious noise, the intensity of the physical signal being too weak. Guided by the analogy with the I0 burst, we can reasonably assume that the dominant wave energy, at least 90%, is contained in the frequency range below 50 Hz, so that the lack of magnetic data above 50 Hz should not modify our conclusions. The integrated electric energies computed from the mean spectra of the I25 (Fig. 11), I27 (Fig. 12), I31 (Fig. 13) and I32 (Fig. 14) bursts are $\simeq 6.8\times10^{-4}$, $\simeq 4.8\times10^{-5}$, $\simeq 5.4\times10^{-5}$, and $\simeq 3.5\times10^{-5}\,(\mathrm{V/m})^2$, respectively. Correspondingly, the integrated magnetic energies computed from the magnetic spectra (<50 Hz), multiplied by 10^5, are $\simeq 9.2\times10^{1}$, $\simeq 1.4\times10^{1}$, $\simeq 1.4\times10^{1}$, and $\simeq 1.8\times10^{1}\,\mathrm{nT}^2$, respectively. Applying (1) and (2) with these numerical values, one gets Poynting flux intensities of $\simeq 2\times10^{-4}$, $\simeq 2\times10^{-5}$, $\simeq 2.2\times10^{-5}$, and $\simeq 2\times10^{-5}\,\mathrm{W/m^2}$, respectively, and E over B ratios of $\simeq 2.7\times10^{6}$, $\simeq 1.8\times10^{6}$, $\simeq 2.0\times10^{6}$, and $\simeq 1.4\times10^{6}\,\mathrm{m/s}$, respectively. Thus, the multiplication by a constant "calibration" factor (10^5) of the magnetic field amplitude gives the same order of magnitude for the E over B ratio as during the I0 flyby, namely, about $2\times10^{6}\,\mathrm{m/s}$. This supports both the existence of a constant calibration factor and its estimated value of about 10^5. This is also consistent with the interpretation that the bursts of wave emissions reported here are the signature of electromagnetic waves that propagate along field lines connected to Io. The same data processing has been carried out for the time interval between the two I27 bursts of wave emissions. One gets for the integrated electric and magnetic mean energies, $(\delta E)^2\simeq 2.2\times10^{-6}\,(\mathrm{V/m})^2$ and $(\delta B)^2\simeq 8.9\,\mathrm{nT}^2$, respectively, which gives a Poynting flux intensity of $\simeq 1.1\times10^{-5}\,\mathrm{W/m^2}$. As a matter of fact, the Poynting flux intensity is of the same order as observed in the adjacent bursts. This is consistent with the picture of incoming waves that strongly slow down as they propagate through an increasingly dense plasma. Further evidence of the effect of a decreasing group velocity can be found in reconsidering the I31 burst. A drop in the electric spectra that coincides with a peak of plasma density is also observed but it is weaker than for the I27 flyby. The fact that this effect is much more pronounced for the I27 flyby can be explained by the particularly large plasma peak density and the particular location of the closest approach. During the I27 flyby, the peak value of the plasma density is actually about 3–4 times larger than for the polar flybys and about double that for the wake crossing. Furthermore, the closest approach was approximately tangential to the Io flux tube at a latitude of 45° off the magnetic equator to Io (Kivelson et al., 2001a). Therefore, the waves observed at the plasma peak density during the I27 flyby must have propagated through an increasingly dense plasma over a longer distance than the waves observed during other flybys.

The energy flux measured during the I25 burst appears to be stronger by an order of magnitude than the I27, I31, and I32 bursts, and by two orders of magnitude than the I0 burst. As mentioned in the overview section, the I25 spectra amplitudes are less reliable than the others. They may be overestimated. Comparing the power densities computed from realtime science data and playback data in the same interval may quantify this assumption. For the I32 flyby, one finds that the mean integrated electric energy is about 4 times larger when it is computed from the realtime science data than when it is computed from the playback data but this factor may vary from case to case. Nevertheless, the case of the I32 flyby shows that the Poynting flux may be overestimated by a factor 4. This would indicate that the I25 burst is still the most intense but only by a factor 2–3. This would give further evidence that the phenomenon reported here is a very systematic one. The fact that the energy flux measured in the I0 burst is one order of magnitude smaller than those observed in other passes may be explained by the relatively large distance from the actual Alfvén wings. In other words, the I0 trajectory did not cross the actual Alfvén wave current system but rather crossed its downstream extended outer edge.

3. Discussion

3.1. On the nature and the origin of the observed waves

Let us now seek to identify the nature of the intense electromagnetic waves that have been systematically observed within the Alfvén wings and in their close vicinity. The protons (f_{H^+}) and typical ion (f_i) gyrofrequencies at Io are $\simeq$30 and $\simeq$1.5 Hz, respectively. The electron inertial length and typical ion Larmor radius are $\sim$100 m and $\sim$3 km, respectively; the Alfvén (v_A) and sound (c_s) speeds are $\sim 1.5\times10^5$ and $\sim 3\times10^4$ m/s, respectively. These values are defined for an unperturbed background torus near Io, namely, for a plasma density $\simeq$4000 cm^{-3}, an ion temperature $\simeq$100 eV, a mean ion atomic number $\simeq$20, an electron temperature $\simeq$ 4 eV, and a magnetic field intensity $\simeq$2000 nT (Frank et al., 1996; Frank and Paterson, 1999; Kivelson et al., 2001a). The frequency range of the plasma waves observed with the PWS instrument extends thus from several f_i to several f_{H^+}; Their E over B ratio ($R_{E/B}$) $\approx 10v_A$. Doppler shift effects due to the relative velocity of the spacecraft with respect to Io ($\simeq$10 km/s) may contribute to the observation of this frequency range. This suggests the possibility of fast magnetosonic waves, proton ion cyclotron waves, or kinetic/inertial Alfvén waves.

The high-frequency (>5 Hz) electromagnetic wave emissions (from PWS) are well correlated with the low-frequency (<2 Hz) magnetic field fluctuations (from the magnetometer). The magnetometer shows a more or less regular succession of incompressible structures where the PWS instrument observes an enhanced electromagnetic broadband noise (up to about 100 Hz). The PWS observations give evidence for a typical integrated (from 5 to 60 Hz) Poynting flux of about 2×10^{-5} W/m^2. Integrating this flux over the Io's cross-section ($\pi R_{Io}^2 \simeq 10^{13}$ m^2) leads to a power of about 2×10^8 W. The average value of the low-frequency (but still small-scale) incompressible magnetic fluctuations observed simultaneously from the magnetometer is about 30 nT. If we interpret them as travelling Alfvénic current structures, taking $v_A \sim 1.5\times10^5$ m/s, one gets a typical value for the Poynting flux of about 1×10^{-4} W/m^2 and a corresponding power of about 1×10^9 W.

This seems to be consistent with the interpretation that the PWS broadband wave emissions and the Alfvénic fluctuations observed with the magnetometer have a common origin. In fact, it may be thought that the PWS instrument simply observes the high-frequency counterpart of the same waves. The origin of these waves is however unclear. Two possibilities can be considered:

(1) The waves are generated directly from Io's ionosphere due to its strongly inhomogeneous conductivity, which leads to diversion of current approximately along the magnetic field. The disturbance propagates outward from Io toward Jupiter. From energy considerations discussed above, these waves are too weak to produce the high-latitude energetic phenomena related to Io.

(2) The waves are the signature of the filamentation/fragmentation of the actual Alfvén wave current system, at some distance from Io. One part is propagating toward Io (where we observe it), the other one, probably the most intense, is propagating toward Jupiter, leading to the formation of intense energetic electron beams.

Let us comment on the first idea.

3.1.1. Wave generation at Io: qualitative aspects

Considering the incompressible fluctuations observed with the magnetometer, the idea of a wave generation at Io from the inhomogeneity of its plasma environment implies that the conductivity of Io's ionosphere and extended ionosphere (as inferred from the I0 flyby) is, to a great extent, strongly non-uniform on a scale size $\leqslant R_{Io}/60 \sim 30$ km. Significant variations over such short distances seem improbable but are possible given that Io may have a patchy atmosphere (Lellouch, 1996; Sartoretti et al., 1994). However, if one also wants to explain the PWS observations, namely the generation of waves up to several times f_{H^+} by the same mechanism, it requires an even much smaller inhomogeneity scale in Io's ionosphere, which is unlikely to occur since the

macroscopic features associated to Io's volcanoes have much larger scale lengths (at least about 100 km).

The currents associated with the Alfvénic fluctuations may drive instabilities as they propagate to higher latitudes. If the parallel current is conserved, the relative drift velocity of the electrons with respect to the ions along the magnetic field increases as one gets into a less dense torus plasma. This relative drift velocity can be of the order of the parallel thermal velocity of the ions, a situation known to be very unstable for small-scale/high frequency waves (Kindel and Kennel, 1971; Forslund et al., 1979). On the other hand, one may object that current driven instabilities should generate waves only in the direction of the relative drift velocity. This means that in the region where the current is flowing downward, no wave should propagate toward Io. However, the PWS instrument observes a systematic presence of wave emissions. The modulation of the downward propagating waves from one upward current region to the other one may, however, not be observed because non-MHD waves are not well-guided and spread out as they propagate toward Io. Additionally, the separation between two adjacent upward current structures may be very small. If this modulation effect were resolved, the only way to understand the observation at Io of a significant fraction of these driven unstable waves (their Poynting flux represents about 20% of the flux radiated by the Alfvénic fluctuations) is to assume a process that couples upward and downward propagating wave modes. This may be possible owing to the parallel and perpendicular inhomogeneities of the small-scale Alfvénic fluctuations as well as of the large-scale Alfvén wave current system.

The idea that the PWS broadband wave emissions originate within the Alfvén wings at some altitude above Io is indeed supported by the fact that these wave emissions are sometimes observed at the outer edge of the actual Alfvén wings and not only within, as it is the case for the low-frequency Alfvénic fluctuations: During the I32 pass, as Galileo crosses the south Alfvén wing from the upstream side, the PWS instrument observes the characteristic broadband wave emissions about one and a half minutes before the magnetometer observes the entry into the Alfvén wing and the simultaneous occurrence of incompressible magnetic fluctuations. This observation can be explained by recognizing that high-frequency waves ($f \geqslant f_i$) are not perfectly guided along the field lines. The same remark can be made for the PWS wave emissions observed outside the Alfvén wing during the low latitude I27 flyby.

3.1.2. Wave generation at Io: quantitative aspects

In this section we further examine, in a quantitative manner, the possible generation at Io of the small-scale incompressible fluctuations observed by the magnetometer. Their typical scale size being much larger than the typical ion Larmor radius and the electron inertial length, an MHD description is used. In particular, we determine an upper bound of their amplitude, as inferred from the basic physics of the Alfvén wings. If they correspond to stationary structures, these small-scale fluctuations observed within the Alfvén wings must be interpreted as spatial fluctuations of the Alfvén wing closure currents. The associated currents thus flow parallel to the axis of the Alfvén wing they originate from and have current densities

$$j_A = \Sigma_A \nabla \cdot (\mathbf{E}) \tag{3}$$

where Σ_A is the Alfvén conductance (Neubauer, 1980). These small-scale standing Alfvén wave currents, like the large-scale Alfvén wing currents, are produced by the diversion of the non-homogeneous current system driven in Io's plasma environment by the corotation electric field ($\mathbf{E}_0$). Writing that the current system at Io is divergence free and then integrating along a path that connects to the corresponding Alfvén wing, one obtains an equation for the electric field. A detailed derivation of this equation is given by Neubauer (1998) in the case of a negligible parallel electric field and a current system at Io consisting of the Pedersen and Hall currents perpendicular to the magnetic field. For the sake of tractability, however, one is generally led to neglect the perturbation/distortion of the magnetic field in this equation (Neubauer, 1998; Saur et al., 1999). This means that one approximates the standing Alfvén wave currents and, the Pederson and Hall currents, respectively, as currents flowing along and perpendicular to the unperturbed magnetic field ($\mathbf{B}_0$). This approximation is valid for a very small Alfvén Mach number ($M_A = v_0/v_A \ll 1$, $\mathbf{v}_0$ being the unperturbed flow velocity) and is thus not fully justified in our case where $M_A \simeq 0.3$. Nevertheless, it must still give the correct order of magnitude of the parameters that govern the physics of the standing Alfvén wave current system at Io. Under these conditions, the equation that determines the electric field, becomes

$$\begin{aligned}(\Sigma_A + \Sigma_P)(\partial_x E_x + \partial_y E_y) \\ + E_x(\partial_x \Sigma_P + \partial_y \Sigma_H) + E_y(\partial_y \Sigma_P - \partial_x \Sigma_H) = 0,\end{aligned} \tag{4}$$

where Σ_P and Σ_H are integrated Pedersen and Hall conductances, respectively, and where the coordinate system used is defined with the y-axis in the direction of $\mathbf{E}_0$ and the z-axis in the direction of $\mathbf{B}_0$, the x-axis pointing mainly along $\mathbf{v}_0$. Provided that the conductances Σ_P and Σ_H are constant inside a circle and null outside, the electric field solution of Eq. (4) is constant inside this circle. For Σ_P or $\Sigma_H \gg \Sigma_A$ this electric field is very small in comparison to E_0, and additionally, strongly tilted toward $\mathbf{v}_0$ if $\Sigma_H \geqslant \Sigma_P$ (Saur et al., 1999). Before going farther, it has to be stressed that the magnetometer observes transverse

fluctuations in both perpendicular directions, and not only in the direction along the unperturbed flow. This indicates that the diversion of the ionospheric current to small-scale Alfvénic currents, if it is the actual process at work, happens not only in the direction along the unperturbed corotation electric field but also along the x-axis. This implies that the inhomogeneity of the integrated Hall conductance, in addition to that of the integrated Pedersen conductance, plays an important role and has to be taken into account.

Let us now consider the constraint given by the measurement of the magnetic fluctuations. Ampere's law implies that in the middle of the standing Alfvén wave current structure

$$j_A \simeq \frac{1}{\mu_0}(\partial_x B_y - \partial_y B_x) \sim \frac{\Delta B}{\mu_0 \Delta L} \tag{5a}$$

with

$$\Delta L = \frac{\Delta x \Delta y}{\Delta x + \Delta y}, \tag{5b}$$

where ΔB is the typical order of magnitude of the associated magnetic field variation, and where Δx and Δy are typical scale lengths that have been introduced for approximating the partial derivatives in the x and y directions, respectively. The definition of the scale length ΔL allows for both cylindrical and plane symmetries. Note that these scale lengths are relevant not only for the magnetic field variations but also for the variations of all other parameters that are coupled with the magnetic field variations. Then, combining Eqs. (3)–(5), one gets an upper bound independent of ΔL for the magnitude of ΔB, that can be produced by the diversion of the Pederson and Hall currents:

$$\Delta B \leqslant \frac{E}{v_A} \frac{\Delta\Sigma_P + \Delta\Sigma_H}{\Sigma_P + \Sigma_A}, \tag{6}$$

where $\Delta\Sigma_P$ and $\Delta\Sigma_H$ represent the order of magnitude of the variation of the conductances Σ_P and Σ_H, respectively. The typical plasma conditions at Io, as inferred from the direct measurements of the plasma flow (Frank et al., 1996; Frank and Paterson, 2001, 2002), from the radio occultation measurement of its plasma wake (Hinson et al., 1998) and from the remote sensing of its interaction with the Jovian corotating plasma (Saur et al., 2000), imply that within the Alfvén wings, on average, $E \leqslant E_0/15$ and $\Sigma_H \sim \Sigma_P \gg \Sigma_A$. Finally, since by definition the typical order of magnitude of the variation of a given parameter cannot exceed its local value, the condition given by Eq. (6) constrains the magnetic fluctuation of a standing Alfvén wave current (located within the large-scale Alfvén wing) to be smaller than about 90 nT, a limit that can be reached only for extremely inhomogeous conditions. This result depends sensibly on the local electric field magnitude E one considers in the middle of the current structure. Here we have used the upper bound of its average value. This deserves some justifications. If one imagines only an increase of the conductances, even very strong, the upper bound of ΔB will actually still be smaller since the local value of E and the relative perturbation ratios will be smaller. This is consistent with the fact that if one starts from a highly conductive plasma, increasing further the conductivity cannot generate much diversion of the currents. On the other hand, if one considers a decrease of the conductances from their average value, the local value of E in the middle of the gradients will be larger. As a result, a larger upper bound of ΔB can be found but for a very strong decrease of the conductances: A 100 nT magnetic fluctuation requires a decrease of the integrated Pedersen and Hall conductances by more than 80%, which in effect means equaling the Alfvén conductance. Note that such extreme conditions are not fulfilled in the gaseous eruptions of Io's volcanoes since the integrated Hall conductance increases with the ion-neutral collision frequency (of course, provided that the electron-neutral collision frequency is still negligible in comparison to the electron gyrofrequency,which is at least fulfilled outside the local regions of dense plumes; Neubauer, 1998). The only way to decrease significantly both the integrated Pedersen and Hall conductances within the Alfvén wings, is to accept the idea of deep drops of the plasma or neutral gas column densities, by about one order of magnitude. Also, as required by the observations, this has to be produced on a typical scale length of only few tens of kilometers, which seems unlikely. Note also that the upper bound of the average electric field magnitude we have used corresponds to a flow velocity inside the Alfvén wings of about 4 km/s, while the PLS observations suggest a smaller velocity (Frank et al., 1996; Frank and Paterson, 2001, 2002). Thus, as a conclusion of this comment, it appears that inhomogeneities of the current system at Io are not able to explain the intense small-scale fluctuations observed by the magnetometer ($\Delta B \sim 100$–150 nT over $\Delta L \sim 20$–40 km), without assuming extreme conditions in the gaseous environment of Io.

3.1.3. Filamentation/fragmentation of the Alfvén wings

Although the interpretation discussed above cannot be absolutely ruled out, we believe that the second possibility, namely a strong dissipation of the Alfvén wing currents, at some distance from Io, is more consistent with the observations. As discussed above, current instabilities may be responsible for the electromagnetic waves observed by the PWS instrument. Here we want to argue that the small-scale Alfvénic currents observed by the magnetometer may also be a by-product of those instabilities, the source of energy being indeed the large-scale Alfvén wing currents. Given the highly

conductive ionosphere of Io, the magnetic field within one Alfvén wing is almost parallel to its axis. The $\sim 3 \times 10^6$ A currents flowing along the large-scale Alfvén wave current tubes are thus almost field-aligned. Assuming that this bipolar current system closes at Io on a surface $\sim \pi R_{\mathrm{Io}}^2/4$, gives an average current density of about $10^{-6}\,\mathrm{A/m^2}$. The parallel drift velocity of the electrons with respect to the ions is thus about 1.5×10^3 m/s, for a $4000/\mathrm{cm}^3$ plasma density in Io's vicinity. At latitudes where the torus plasma is 10 times less dense, namely at about 1–2 Jupiter radii from Io (Bagenal et al., 1997), this drift velocity may match the ion thermal speed. The standing Alfvén wave current system may thus be strongly destabilized by current driven instability just before it encounters the sharp torus boundary gradient that reflects it (Wright and Schwartz, 1989; Crary, 1997). Furthermore, it has to be stressed that the density of the Alfvén wing current is of the order of those observed within the small-scale Alfvénic currents detected by the magnetometer. As a result, even in the framework of the first interpretation, one is led to admit that the actual Alfvén wing current system is likely to be destabilized. With this possibility in mind, we propose to interpret the intense broadband wave activity observed systematically during the crossing of the Alfvén wings as the signature of their filamentation/fragmentation into "high-frequency/small-scale" electromagnetic waves. Also, it has to be stressed that by filamentation/fragmentation one requires the creation of small-scale structures inside the whole Alfvén wing volume and not only filamentation of the currents on its edge. This may happen since the Alfvén wing at Io is a three-dimensional structure, which differs much from a one-dimensional plane wave. In fact, as initiated by current instabilities, the filamentation of the large-scale Alfvén wave currents is perhaps the first step of the filamentation/fragmentation process we propose here for explaining the observations.

3.2. On the process of electron acceleration by Io

The present work aims to identify, mainly from the plasma wave observations, the key steps of the process that generates the energetic electrons responsible for the Io-related phenomena at high-latitudes. Crary (1997) has proposed an analytic model showing that an intense electron beam can form in front of the Alfvén wings by repeated Fermi acceleration. The model considers the propagation of an impulsive Alfvénic disturbance through the non-uniform background torus of Io, from Io toward Jupiter. Most of the Alfvénic disturbance is indeed reflected owing to the strong variation of the Alfvén speed or, in other words, owing to the fact that the typical wavelength of the disturbance becomes larger than the scale height of the torus boundary (the WKB approximation breaks down at about 1.5 Jupiter radii from Io). Thus, most of the magnetic energy should not reach Jupiter's ionosphere. It is therefore difficult to understand how the actual large-scale Alfvénic structure can trap electrons and accelerate them to the required energy. Modeling the Io-torus interaction as an impulsive disturbance inevitably introduces high frequencies in the wave spectrum and, as a consequence, overestimates the magnitude of the parallel electric field and underestimates the wave reflection. Furthermore, since the Alfvén disturbance is strongly accelerated during its propagation through the Io torus, the non-Galilean force cannot be neglected in the Fermi acceleration process. Comparing the parallel electric force,

$$qE_{\parallel} \simeq \frac{q\omega j_{\parallel}}{\varepsilon_0\,\omega_{\mathrm{pe}}^2(z=0)} \sim 2 \times 10^{-28}\,\mathrm{N}, \tag{7}$$

with the non-Galilean force experienced by an electron in the Alfvén wave's frame of reference,

$$F_{\mathrm{a}} \simeq m v_{\mathrm{A}}^2(z=0)/R_{\mathrm{J}} \sim 5 \times 10^{-28}\,\mathrm{N}, \tag{8}$$

one concludes that the actual large-scale Alfvén wing cannot trap electrons during its accelerated propagation toward Jupiter. For the numerical estimates we have considered the typical time scale of the Alfvénic disturbance, as given by the time Io takes to sweep Jupiter's field lines, thus $\omega \sim 2\pi/60$ Hz. Otherwise, we have used conditions similar to those used by Crary (1997), namely, $\omega_{\mathrm{pe}}(z=0) \sim 2\pi\,5 \times 10^5$ Hz, $j_{\parallel} \sim 10^{-6}\,\mathrm{A/m^2}$, and an exponential dependence of the Alfvén speed on the distance along the field line, where $v_{\mathrm{A}}(z=0) \sim 2 \times 10^5$ m/s and the scale height is about one Jupiter radius, $R_{\mathrm{J}} \simeq 70000$ km.

The observation of bidirectional field-aligned 100 keV electrons at Io (Williams et al., 1996, 1999; Mauk et al., 2001) gives some useful support to the interpretation that we propose. If resonant wave–particle interaction is the primary dissipation process, only waves propagating at almost a relativistic speed are able to accelerate electrons to such energies. This seems possible only at high latitudes, outside the Io torus, where the Alfvén speed reaches its relativistic limit. The observations reported here contribute precious information to resolve this issue. The fact that the Alfvén wings cannot extend significantly outside the Io plasma torus and that an intense broadband wave activity at Io is systematically associated with them, indicates that a transfer of energy from the large-scale Alfvén wave current system into "high-frequency/small-scale" electromagnetic waves must occur within the torus. The time scales observed for the broadband wave activity (less than 2 s) being much smaller than the time scale of the standard Alfvénic disturbance (at least 60 s), the corresponding wavelengths are most probably much smaller than the scale height of the torus boundary. The "high-

frequency/small-scale'' waves generated and travelling toward Jupiter propagate therefore approximately in a WKB manner and do not sense the torus boundary gradient significantly. They can thus reach high-latitude in Jupiter's magnetosphere where they can be strongly damped by accelerating electrons to the required energy and flux. Various acceleration mechanisms can then be considered. For instance, one may consider again the repeated Fermi acceleration process, as proposed by Crary (1997) (but apply it to the high frequency part of the waves), the non-linear evolution of anomalous resistivity (Kopp et al., 1998), or even more complicated features such as the non-linear mode conversion into kinetic Alfvén waves (Das and Ip, 2000). The identification of the specific wave–particle interaction at work is beyond the scope of this paper. One may however retain that the general concept of non-linear trapping in a non-uniform medium is the most plausible paradigm for explaining the energetic electron beams observed in the Io flux tube.

Thus the formation of energetic electron beams by Io requires some time, namely the time the ''high-frequency/small-scale'' waves generated toward Jupiter take to reach the high-latitude Jovian magnetosphere. In order to observe part of these beams at Io, the time needed for their adiabatic reflection has to be added. During that time, the Io field lines drift slowly downstream. Energetic electron beams are therefore not expected in the upstream region. On the other hand, the ''high-frequency/small-scale'' waves propagating toward Io (those we observe), even though they are much less intense than those propagating away from Io toward Jupiter, can also accelerate electrons. Since these waves are expected to propagate slowly (small value of the Alfvén speed within the Io torus), the electrons interacting with them cannot reach high energies. However, they may be present in the upstream region. The fact that an electron beam was observed during the upstream I27 flyby with the PLS instrument (>8 eV) and not with the EPD instrument (>15 keV), is consistent with this picture.

4. Conclusion

The observations reported here show that the Alfvén wave current system at Io is systematically associated with an intense electromagnetic wave activity, located within the whole cross-section of the Alfvén wings and in their immediate vicinity. The frequency range of the waves extends from below f_i to several f_{H^+}. We interpret them as the signature of a strong filamentation/fragmentation of the Alfvén wings before their first reflection by the sharp torus boundary. It is thus suggested that a continuous energy transfer from the large-scale Alfvén wave current system into ''high-frequency/small-scale'' electromagnetic waves occurs prior to any significant electron acceleration process. From the energy balance between the power emitted by Io into the Alfvén wings and the power consumed by the Io-related high latitude phenomena, the energy transfer coefficient may be as large as 50%. The ''high-frequency/small-scale'' electromagnetic waves that propagate toward Jupiter are effectively less reflected by the torus boundary and can thus reach the high-latitude magnetophere where they can accelerate electrons to almost relativistic speeds and be completely dissipated before reaching Jupiter's ionosphere. In order to describe the quantitative aspects of this three-step process, a non-linear kinetic treatment of the Alfvén wings in a non-uniform medium is necessary. Our interpretation of the high-frequency, small scale structure of the current system near Io explains how significant power can penetrate the reflecting boundary at the outer edge of the plasma torus and provides a new picture of the Io–Jupiter interaction region.

Acknowledgements

We are grateful to G. Belmont for the many fruitful discussions. The French participation in this work is supported by CNRS and CNES. The research at the University of Iowa was supported by NASA through contract 958779 with the Jet Propulsion Laboratory. This research was also supported by the Jet Propulsion Laboratory under contract JPL 1238965.

References

Acuna, M.H., Neubauer, F.M., Ness, N.F., 1981. Standing Alfvén wave current system at Io: Voyager-1 observations. J. Geophys. Res. 86, 8513.

Bagenal, F., Crary, F.J., Stewart, A.I.F., Schneider, N.M., Gurnett, D.A., Kurth, W.S., Frank, L.A., Paterson, W.R., 1997. Galileo measurements of plasma density in the Io torus. Geophys. Res. Lett. 24, 2119.

Bigg, E.L., 1964. Influence of the satellite Io on Jupiter's decametric radiation. Nature 203, 1008.

Chust, T., Roux, A., Perraut, S., Louarn, P., Kurth, W.S., Gurnett, D.A., 1999. Galileo plasma wave observations of iogenic hydrogen. Planet. Space Sci. 47, 1377.

Clarke, J.T., Ballester, G.E., Trauger, J., Evans, R., Connerney, J.E.P., Stapelfeldt, K., Crisp, D., Feldman, P.D., Burrows, C.J., Casertano, S., Gallagher III, J.S., Griffiths, R.E., Hester, J.J., Hoessel, J.G., Hotzman, J.A., Krist, J.E., Meadows, V., Mould, J.R., Scowen, P.A., Watson, A.M., Westphal, J.A., 1996. Far-ultraviolet imaging of Jupiter's aurora and Io ''footprint''. Science 274, 404.

Clarke, J.T., Ballester, G., Trauger, J., Ajello, J., Prior, W., Tobiska, K., Connerney, J.E.P., Gladstone, G.R., Waite Jr., J.H., Jaffel, L.B., Gérard, J.C., 1998. Hubble space telescope imaging of Jupiter's UV aurora during the Galileo orbiter mission. J. Geophys. Res. 103, 20217.

Connerney, J.E.P., Baron, R., Satoh, T., Owen, T., 1993. Images of excited H_3^+ at the foot of the Io flux tube in Jupiter's atmosphere. Science 262, 1035.

Crary, F.J., 1997. On the generation of an electron beam by Io. J. Geophys. Res. 102, 37.
Crary, F.J., Bagenal, F., 1997. Coupling the plasma interaction at Io to Jupiter. Geophys. Res. Lett. 24, 2135.
Das, A.C., Ip, W.-H., 2000. Field aligned current and particle acceleration in the near-Io plasma torus. Planet. Space Sci. 48, 127.
Delory, G.T., Ergun, R.E., Carlson, C.W., Muschietti, L., Chaston, C.C., Peria, W., McFadden, J.P., Strangeway, R., 1998. FAST observations of electron distributions within AKR source regions. Geophys. Res. Lett. 25, 2069.
Drell, S.D., Foley, H.M., Ruderman, M.A., 1965. Drag and propulsion of large satellites in the ionosphere: an Alfvén propulsion engine in space. J. Geophys. Res. 70, 3131.
Forslund, D.W., Kindel, J.M., Stroscio, M.A., 1979. Current driven electromagnetic ion cyclotron instability. J. Plasma Phys. 21, 127.
Frank, L.A., Paterson, W.R., 1999. Intense electron beams observed at Io with the Galileo spacecraft. J. Geophys. Res. 104, 28657.
Frank, L.A., Paterson, W.R., 2000. Return to Io by the Galileo spacecraft: plasma observations. J. Geophys. Res. 105, 25363.
Frank, L.A., Paterson, W.R., 2001. Passage through Io's ionospheric plasmas by the Galileo spacecraft. J. Geophys. Res. 106, 26209.
Frank, L.A., Paterson, W.R., 2002. Plasmas observed with the Galileo spacecraft during its flyby over Io's northern polar region. J. Geophys. Res. 107, SMP 31–1.
Frank, L.A., Paterson, W.R., Ackerson, K.L., Vasyliunas, V.M., Coroniti, F.V., Bolton, S.J., 1996. Plasma observations at Io with the Galileo spacecraft. Science 274, 394.
Goertz, C.K., Deift, P.A., 1973. Io's interaction with the magnetosphere. Planet. Space Sci. 21, 1399.
Goldreich, P., Lynden-Bell, D., 1969. Io, a Jovian unipolar inductor. Astrophys. J. 156, 59.
Gurnett, D.A., Kurth, W.S., Shaw, R.R., Roux, A., Gendrin, R., Kennel, C.F., Scarf, F.L., Shawhan, S.D., 1992. The Galileo plasma wave investigation. Space Sci. Rev. 60, 341.
Gurnett, D.A., Persoon, A.M., Kurth, W.S., Roux, A., Bolton, S.J., 2001. Electron densities near Io from Galileo plasma wave observations. J. Geophys. Res. 106, 26225.
Hill, T.W., Pontius Jr., D.H., 1998. Plasma injection near Io. J. Geophys. Res. 103, 19879.
Hill, T.W., Dessler, A.J., Goertz, C.K., 1983. Magnetospheric models. In: Dessler, A.J. (Ed.), Physics of the Jovian Magnetosphere. Cambridge University Press, New York.
Hinson, D.P., Kliore, A.J., Flasar, F.M., Twicken, J.D., Schinder, P.J., Herrera, R.G., 1998. Galileo radio occultation measurements of Io's ionosphere and plasma wake. J. Geophys. Res. 103, 29,343.
Huddleston, D.E., Strangeway, R.J., Warnecke, J., Russell, C.T., Kivelson, M.G., Bagenal, F., 1997. Ion cyclotron waves in the Io torus during the Galileo encounter: warm plasma dispersion analysis. Geophys. Res. Lett. 24, 2143.
Huddleston, D.E., Strangeway, R.J., Warnecke, J., Russell, C.T., Kivelson, M.G., 1998. Ion cyclotron waves in the Io torus: wave dispersion, free energy analysis, and SO_2^+ source rate estimates. J. Geophys. Res. 103, 19887.
Huddleston, D.E., Strangeway, R.J., Blanco-Cano, X., Russell, C.T., Kivelson, M.G., Khurana, K.K., 1999. Mirror-mode structures at the Galileo-Io flyby: instability criterion and dispersion analysis. J. Geophys. Res. 104, 17479.
Kindel, J.M., Kennel, C.G., 1971. Topside current instabilities. J. Geophys. Res. 76, 3055.
Kivelson, M.G., Khurana, K.K., Walker, R.J., Russell, C.T., Linker, J.A., Southwood, D.J., Polanskey, C., 1996a. A magnetic signature at Io: initial report from the Galileo magnetometer. Science 273, 337.
Kivelson, M.G., Khurana, K.K., Walker, R.J., Warnecke, J., Russell, C.T., Linker, J.A., Southwood, D.J., Polanskey, C., 1996b. Io's interaction with the plasma torus: Galileo magnetometer report. Science 274, 396.
Kivelson, M.G., Khurana, K.K., Russell, C.T., Joy, S.P., Volwerk, M., Walker, R.J., Zimmer, C., Linker, J.A., 2001a. Magnetized or unmagnetized: ambiguity persists following Galileo's encounters with Io in 1999 and 2000. J. Geophys. Res. 106, 26121.
Kivelson, M.G., Khurana, K.K., Russell, C.T., Walker, R.J., 2001b. Magnetic signature of a polar pass over Io. Eos Trans. AGU 82 (47) (Fall Meet. Suppl.) (Abstract P11A-01).
Kopp, A., Birk, G.T., Otto, A., 1998. On the formation of Io-related Jovian discrete auroral phenomena. Adv. Space Res. 21, 1469.
Lellouch, E., 1996. Io's atmosphere: not yet understood. Icarus 124, 1.
Linker, J.A., Kivelson, M.G., Walker, R., 1988. An MHD simulation of plasma flow past Io: Alfvén and slow mode perturbations. Geophys. Res. Lett. 15, 1311.
Linker, J.A., Kivelson, M.G., Walker, R., 1991. A three-dimensional MHD simulation of plasma flow past Io. J. Geophys. Res. 96, 21037.
Louarn, P., Roux, A., de Feraudy, H., Le Quéau, D., André, M., Matson, L., 1990. Trapped electrons as a free energy source for the auroral kilometric radiation. J. Geophys. Res. 95, 5983.
Mauk, B.H., 2001. Over Io's poles: energetic particle results. AGU, Fall Meeting, P11A-02.
Mauk, B.H., Williams, D.J., Eviatar, A., 2001. Understanding Io's space environment interaction: recent energetic electron measurements from Galileo. J. Geophys. Res. 106, 26195.
Neubauer, F.M., 1980. Nonlinear standing Alfvén wave current system at Io: theory. J. Geophys. Res. 85, 1171.
Neubauer, F.M., 1998. The sub-Alfvénic interaction of the Galilean satellites with the Jovian magnetosphere. J. Geophys. Res. 103, 19843.
Paterson, W.R., Frank, L.A., 2002a. The Plasma environment and electron beams at Io. AGU, Spring Meeting, P21B-02.
Paterson, W.R., Frank, L.A., 2002b. Auroral electron beams in the Jovian magnetosphere. AGU, Fall Meeting, SM21A-0523.
Piddington, J.H., Drake, J.F., 1968. Electrodynamic effects of Jupiter's satellite Io. Nature 217, 935.
Prangé, R., Rego, D., Southwood, D., Zarka, P., Miller, S., Ip, W., 1996. Rapid energy dissipation and variability of the Io–Jupiter electrodynamic circuit. Nature 379, 323.
Prangé, R., Rego, D., Pallier, L., Connerney, J.E.P., Zarka, P., Queinnec, J., 1998. Detailed study of FUV Jovian auroral features with the post-COSTAR HST faint object camera. J. Geophys. Res. 103, 20195.
Queinnec, J., Zarka, P., 1998. Io-controlled decameter arcs and Io–Jupiter interaction. J. Geophys. Res. 103, 26649.
Queinnec, J., Zarka, P., 2001. Flux, power, energy and polarization of Jovian S-bursts. Planet. Space Sci. 49, 365.
Russell, C.T., Huddleston, D.E., Strangeway, R.J., Blanco-Cano, X., Kivelson, M.G., Frank, L.A., Paterson, W., Gurnett, D.A., Kurth, W.S., 1999. Mirror-mode structures at the Galileo-Io flyby: observations. J. Geophys. Res. 104, 17471.
Sartoretti, P., McGrath, M.A., Paresce, F., 1994. Disk-resolved imaging of Io with the Hubble space telescope. Icarus 108, 272.
Saur, J., Neubauer, F.M., Strobel, D.F., Summers, M.E., 1999. Three-dimensional plasma simulation of Io's interaction with the Io plasma torus: asymmetric plasma flow. J. Geophys. Res. 104, 25105.
Saur, J., Neubauer, F.M., Strobel, D.F., Summers, M.E., 2000. Io's ultraviolet aurora: remote sensing of Io's interaction. Geophys. Res. Lett. 27, 2893.
Vasavada, A.R., Bouchez, A.H., Ingersoll, A.P., Little, B., Anger, C.D., The Galileo SSI Team, 1999. Jupiter's visible aurora and Io footprint. J. Geophys. Res. 104, 27133.
Warnecke, J., Kivelson, M.G., Khurana, K.K., Huddleston, D.E., Russell, C.T., 1997. Ion cyclotron waves observed at Galileo's Io

encounter: implications for neutral cloud distribution and plasma composition. Geophys. Res. Lett. 24, 2139.
Warwick, J.W., 1981. Models for Jupiter's decametric arcs. J. Geophys. Res. 86, 8585.
Williams, D.J., Mauk, B.H., McEntire, R.E., Roelof, E.C., Amstrong, T.P., Wilken, B., Roederer, J.G., Krimigis, S.M., Fritz, T.A., Lanzerotti, L.J., 1996. Electron beams and Ion composition measured at Io and in its torus. Science 274, 401.
Williams, D.J., Thorne, R.M., Mauk, B.H., 1999. Energetic electron beams and trapped electrons at Io. J. Geophys. Res. 104, 14739.
Wright, A.N., Schwartz, S., 1989. The transmission of Alfvén waves through the Io plasma torus. J. Geophys. Res. 94, 3749.
Wright, A.N., Schwartz, S., 1990. The equilibrium of a conducting body embedded in a flowing plasma. J. Geophys. Res. 95, 4027.
Zarka, P., Farges, T., Ryabov, B.P., Abada-Simon, M., Denis, L., 1996. A scenario for Jovian S-bursts. Geophys. Res. Lett. 23, 125.
Zarka, P., Queinnec, J., Crary, F.J., 2001. Low-frequency limit of Jovian radio emissions and implications on source locations and Io plasma wake. Planet. Space Sci. 49, 1137.